



# HHS Public Access

Author manuscript

Cell Rep. Author manuscript; available in PMC 2019 June 20.

Published in final edited form as:

Cell Rep. 2019 May 14; 27(7): 2014–2021.e2. doi:10.1016/j.celrep.2019.04.069.

## Independent Contributions of Discrete Dopaminergic Circuits to Cellular Plasticity, Memory Strength, and Valence in *Drosophila*

Tamara Boto<sup>1</sup>, Aaron Stahl<sup>1</sup>, Xiaofan Zhang<sup>1</sup>, Thierry Louis<sup>1</sup>, and Seth M. Tomchik<sup>1,2,\*</sup>

<sup>1</sup>Department of Neuroscience, The Scripps Research Institute, Jupiter, FL 33458, USA

<sup>2</sup>Lead Contact

### SUMMARY

Dopaminergic neurons play a key role in encoding associative memories, but little is known about how these circuits modulate memory strength. Here we report that different sets of dopaminergic neurons projecting to the *Drosophila* mushroom body (MB) differentially regulate valence and memory strength. PPL2 neurons increase odor-evoked calcium responses to a paired odor in the MB and enhance behavioral memory strength when activated during olfactory classical conditioning. When paired with odor alone, they increase MB responses to the paired odor but do not drive behavioral approach or avoidance, suggesting that they increase the salience of the odor without encoding strong valence. This contrasts with the role of dopaminergic PPL1 neurons, which drive behavioral reinforcement but do not alter odor-evoked calcium responses in the MB when stimulated. These data suggest that different sets of dopaminergic neurons modulate olfactory valence and memory strength via independent actions on a memory-encoding brain region.

### Graphical Abstract

---

This is an open access article under the CC BY-NC-ND license (<http://creativecommons.org/licenses/by-nc-nd/4.0/>).

\*Correspondence: [stomchik@scripps.edu](mailto:stomchik@scripps.edu).

#### AUTHOR CONTRIBUTIONS

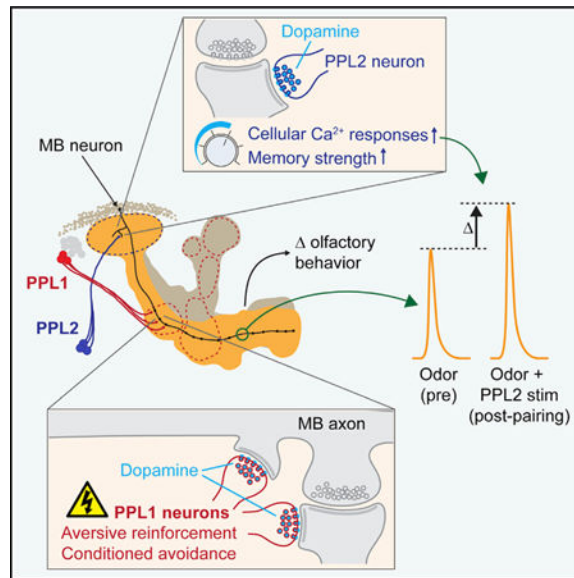
Conceptualization, T.B. and S.M.T.; Methodology, T.B., A.S., X.Z., and T.L.; Investigation, T.B., A.S., X.Z., and T.L.; Supervision, S.M.T.; Writing, T.B. and S.M.T.; Project Administration, S.M.T.; Funding Acquisition, S.M.T.

#### SUPPLEMENTAL INFORMATION

Supplemental Information can be found online at <https://doi.org/10.1016/j.celrep.2019.04.069>.

#### DECLARATION OF INTERESTS

The authors declare no competing interests.



## In Brief

Boto et al. investigated the roles of two sets of dopaminergic neurons that converge on a memory-encoding brain region in flies. While one set, PPL1, drives aversive reinforcement (valence), PPL2 neurons enhance memory strength via modulation of Ca<sup>2+</sup> response plasticity in memory-encoding mushroom body neurons.

## INTRODUCTION

Dopaminergic neurons are involved in associative learning across taxa (Schultz, 1997; Schwaerzel et al., 2003; Matsumoto and Hikosaka, 2009; Liu et al., 2012a). In *Drosophila*, activation of certain dopaminergic neurons during associative learning tasks drives conditioned approach or avoidance, suggesting that they function as part of the reinforcement pathway and may encode stimulus valence (positive or negative) (Schroll et al., 2006; Claridge-Chang et al., 2009; Aso et al., 2010, 2012; Liu et al., 2012a; Yamagata et al., 2015). There are eight clusters of dopaminergic neurons in the fly brain (Tanaka et al., 2008; Mao and Davis, 2009). Neurons in three clusters project to the mushroom body (MB), a region that receives olfactory information and is required for olfactory learning. PAM dopaminergic neurons project to the horizontal lobes ( $\beta$ ,  $\beta'$ , and  $\gamma$ ); PPL1 neurons project to the vertical lobes ( $\alpha$  and  $\alpha'$ ), heel, and peduncle; and PPL2ab neurons project to the calyx (Figure 1A). Different subsets of PPL1 and PAM neurons modulate reinforcement during learning (Schroll et al., 2006; Claridge-Chang et al., 2009; Aso et al., 2010; Berry et al., 2012).

Different sets of dopaminergic neurons play discrete roles in reinforcement during learning. Activating PPL1 dopaminergic neurons in lieu of reinforcement induces behavioral aversion to a paired odor (Schroll et al., 2006; Claridge-Chang et al., 2009; Aso et al., 2010, 2012). Conversely, activation of PAM neurons is sufficient to generate appetitive memories (Liu et al., 2012a; Yamagata et al., 2015). These dopaminergic neurons respond strongly to the

unconditioned stimulus during conditioning, releasing dopamine into the MB that integrates with odorevoked spiking activity to drive learning-induced, cyclic AMP (cAMP)-dependent plasticity in the MB (Riemensperger et al., 2005; Mao and Davis, 2009; Tomchik and Davis, 2009; Gervasi et al., 2010; Boto et al., 2014; Louis et al., 2018). Little is known about the third MB-innervating cluster, PPL2ab. These neurons innervate the ipsilateral MB calyx, as well as the lateral horn, lobula, optical track and esophagus, and medial and posterior protocerebrum (Tanaka et al., 2008; Mao and Davis, 2009). They have been implicated in the regulation of courtship behaviors (Kuo et al., 2015; Chen et al., 2017) but have no known role in learning and memory. How the multiple dopaminergic circuits that converge on the MB regulate learning is a major question.

We have investigated the distinct roles of MB-innervating dopaminergic circuits in neuronal plasticity and behavioral memory. We found that PPL2 neurons play a role in learning, modulating neuronal gain and memory strength without imparting a strong valence. Thus, different subsets of dopaminergic neurons converging on memory-encoding neurons (the MB neurons) play roles in modulation of memory strength and valence.

## RESULTS

### Stimulation of Dopaminergic Neurons Increases MB Calcium Responses to Odors in an Associative Manner

Dopaminergic neurons labeled by the tyrosine hydroxylase Gal4 (TH-Gal4) driver are sufficient to drive aversive reinforcement in classical conditioning (Schroll et al., 2006; Claridge-Chang et al., 2009; Aso et al., 2010, 2012) and produce calcium response plasticity in the MB g lobe when stimulated with odor presentation (Boto et al., 2014). This driver includes three sets of MB-innervating neurons: PPL1, PPL2ab, and PAM (M3) neurons (Figure 1A; Tanaka et al., 2008; Mao and Davis, 2009; Aso et al., 2014a). The time course and subsets of dopaminergic neurons underlying the effect on MB plasticity are unknown. To examine this, we imaged odor-evoked  $Ca^{2+}$  responses in the MB  $\gamma$  lobe with GCaMP (Figures 1A and 1B), and stimulated TH-Gal4<sup>+</sup> neurons with UAS-TrpA1. Odor was paired with stimulation of TH-Gal4<sup>+</sup> dopaminergic neurons, ramping the temperature to activate TrpA1 in a conditioning paradigm (Figures 1C and 1D).

Pairing odor with stimulation of TH-Gal4<sup>+</sup> neurons generated an increase in MB  $\gamma$  lobe  $Ca^{2+}$  responses to the odor with forward relative to backward conditioning (Figures 1E and 1G), in agreement with our previous data (Boto et al., 2014). This plasticity was present at 5 min following conditioning and gone by 60 min (Figure 1H), suggesting that it is associated with short-term memory. When two odors were presented in a differential conditioning paradigm,  $Ca^{2+}$  responses to the trained odor (conditioned stimulus [CS]<sup>+</sup>) were enhanced relative to those to the untrained odor (CS<sup>-</sup>) (Figures 1E–1G). The plasticity was consistent across two trained odors, ethyl butyrate (EB) and isoamyl acetate (IA) (Figure 1G). We observed increases in the trained odor (forward, CS<sup>+</sup>) and decreases in the untrained odor (backward, CS<sup>-</sup>) responses. However, in a previous study, we found that presentation of odor for 30 s during training produces sensory adaptation that presumably underlies the apparent CS<sup>-</sup> effect (Louis et al., 2018). This suggested that the reduction in backward and CS<sup>-</sup> groups observed here was likely due to nonassociative adaptation and that training

increased the forward or CS+ odor responses on top of this baseline. To test this, we imaged animals in which an odor was presented for 30 s with no reinforcement (adaptation, Figures 1I–1K; odor only, Figure 2I) and found an equivalent drop in responses to CS– (responses to a third odor were unaffected by conditioning) (Figures 1I–1K).

### Dopaminergic Plasticity at the Cellular Level Maps to PPL2, Not PPL1, Neurons

Although PPL1 neurons innervate mainly the vertical lobes, PPL2ab neurons innervate the MB dendrites in the calyces (Mao and Davis, 2009; Figures 1A and 2A–2E). To parse the effects of these subdivisions on MB plasticity, we separated the PPL1 and PPL2ab neurons with more restricted Gal4 drivers: TH-D'-Gal4 for PPL1 neurons (Figures 2A and 2B; Liu et al., 2012b) and TH-C'-Gal4 combined with the F-Gal80 repressor for PPL2 (Figures 2C–2E). We henceforth refer to these drivers as PPL1-Gal4 and PPL2-Gal4, respectively.

PPL1 neurons are necessary for aversive reinforcement processing in the MB (Schwaerzel et al., 2003; Berry et al., 2012). Therefore, if the increase in odor-evoked Ca<sup>2+</sup> responses represents the effect of acquired aversive valence, the plasticity would map to PPL1 neurons. To test this, we examined changes in odor representation when odor was paired with PPL1 or PPL2 stimulation in a differential conditioning paradigm. Pairing odor with PPL1 stimulation produced no significant cellular Ca<sup>2+</sup> plasticity in the MB g lobe, using either forward versus backward or differential conditioning (Figures 2F and 2G). In contrast, pairing PPL2 activation with olfactory stimulation induced facilitation of odorevoked responses in the g lobe (Figures 2H and 2I). We also tested additional drivers that label varying numbers of PPL2 neurons (Figures 2J–2N and S4J; Blanco et al., 2011; Kuo et al., 2015). Stimulating PPL2 neurons with all tested drivers produced detectable plasticity in the MB g lobe (Figures 2J–2N). However, the PPL2-Gal4 driver, which labels the largest number of PPL2 neurons, drove the strongest plasticity (Figures 2I–2N). Overall, these data demonstrate that the PPL2 subset of TH+ dopaminergic neurons is responsible for the cellular-level Ca<sup>2+</sup> response plasticity observed in the MB  $\gamma$  lobes.

Odor-evoked responses imaged in the MB lobes represent the summed activity of hundreds of neurons. To determine how PPL2 stimulation affects individual neurons, we imaged individual somata in the MB (Figures S1A–S1E). Because MB neurons respond sparsely to any odorant (Figure S1B; Turner et al., 2008), only odor-responsive neurons were included in the analyses. Odor-evoked responses were compared before and after pairing an odor with PPL2 stimulation in a differential conditioning paradigm (Figure S1C). Individual MB neurons exhibited increased CS+ responses relative to CS— responses (Figures S1D and S1E).

PPL2 neurons innervate the dendrites of the MB neurons in the calyx region. To test whether the plasticity was present in the dendrites, we carried out differential conditioning experiments while imaging the calyx (Figures S1F and S1G). Pairing odor with activation of either TH-Gal4+ or the PPL2 subset alone produced plasticity in the MB calyx (Figure S1G). In contrast, stimulation of PPL1 neurons produced no significant changes. A previous study failed to detect dopamine-dependent plasticity in the  $\alpha$  lobe with TH-Gal4+ neuron stimulation (Boto et al., 2014). Here we tested whether PPL2 activation produced plasticity in the MB  $\alpha$  lobe and similarly found no significant change (Figures S1H–S1J). Altogether,

these data suggest that dopamine-dependent plasticity at the dendritic inputs produces associative plasticity in  $\text{Ca}^{2+}$  responses in MB  $\gamma$  neurons. This may represent a more modulatory contribution to memory than the heterosynaptic plasticity driven in the MB lobes by PPL1 neurons, a hypothesis we consider further later.

### **PPL2 Neurons Respond to Odor and Shock but Do Not Encode Strong Valence**

The observation of PPL2-driven plasticity suggested that these neurons may be activated during learning. To test this, we imaged PPL2 responses to electric shock and odors in the calyx and/or somata regions (Figure 3A). PPL2 somata showed increases in  $\text{Ca}^{2+}$  when the flies were stimulated with 60-V electric shocks under the microscope (Figure 3B). In addition, they responded to EB and IA (Figure 3C). These odor responses were observed both in PPL2 somata and in PPL2 projections in the MB calyx (Figures S2A and S2B). Among PPL2 somata, some individual neurons responded to odors, while others did not (Figure S2B).

The preceding data suggest that PPL2 neurons exert strong effects on MB physiology, potentially increasing the gain of the MB responses to a paired odor. This raises the question of what behavioral role PPL2 neurons play. We first tested whether stimulating PPL2 neurons imparts valence on a paired odor using a reinforcement substitution paradigm (Figure 3D). Pairing odor with stimulation of PPL1 neurons produced aversive memory, in agreement with previous studies (Riemensperger et al., 2005; Schroll et al., 2006; Claridge-Chang et al., 2009; Aso et al., 2012). In contrast, pairing odor with PPL2 stimulation produced no significant memory (Figure 3E). This suggests that PPL2 neurons do not convey a major reinforcement signal to the MB and thus have a distinct behavioral function from PPL1 (and PAM) neurons.

### **PPL2 Neurons Modulate Memory Strength**

Because PPL2 neurons exerted strong effects on odor-evoked responses in the MB but did not drive valence, we questioned whether they modulate memory strength. To test this, we examined behavioral memory using a weak aversive training paradigm. Odor was paired with  $3 \times 60\text{-V}$  shocks over 1 min, in place of the typical  $12 \times 90\text{-V}$  protocol that produces ceiling-level performance. This was paired with activation of PPL2 neurons at various times during the protocol (Figure 4A). Flies expressing TrpA1 in PPL2 neurons were compared to genetic controls. When the PPL2 neurons were stimulated during odor-shock pairing (during CS+ presentation), performance was significantly elevated, representing an increase in memory strength. The effect was observed with two odor pairs: EB versus IA (Figure 4B) and 3-octanol (Oct) versus methylcyclohexanol (Mch) (Figure 4C). These effects could not be explained by changes in odor or shock sensitivity (Table S1).

To delineate the temporal requirements for PPL2-induced memory enhancement, we ran additional conditioning experiments using the IA-EB odor pair. No enhancement of memory was observed when stimulating PPL2 neurons at times outside the presentation of CS+ exclusively (Figures 4D–4H). Performance was lower in all genotypes when pairing heat with CS— (Figure 4D), likely due to reinforcement from the heat (Galili et al., 2014). No effect was observed when heat was omitted (Figure 4I). Finally, to address the specificity of

dopaminergic circuitry within the PPL2-Gal4 driver, we introduced a TH-Gal80 repressor to subtract dopaminergic neurons from the expression pattern (Sitaraman et al., 2008). When the expression of TrpA1 in dopaminergic neurons was suppressed, the enhancement of aversive memory performance disappeared (Figure 4J). These data suggest that PPL2 neurons modulate relative memory strength when active during learning.

We next tested whether stimulation of PPL2 neurons during classical conditioning produced different physiological effects from pairing PPL2 stimulation with odor alone (Figures S2C–S2E). Odor responses were imaged before and after pairing CS+ with TrpA1 activation, and electric shock was delivered to the legs and/or abdomen (Louis et al., 2018). Responses were recorded in the  $\gamma$  lobe, and the results were compared across four protocols (Figure S2C). Pairing PPL2 stimulation with an odor increased the relative responses to the paired odor, regardless of whether shocks were also paired (Figures S2D and S2E). Pairing odor with electric shock alone produced no change in MB  $\gamma$  lobe responses (Figure S2E), consistent with our previous data (Louis et al., 2018). Thus, PPL2 stimulation enhances MB responses to a paired odor, and there was no detectable interaction with electric shock.

To test for loss of function phenotypes, we blocked synaptic output of PPL2 neurons using *shibire<sup>ts</sup>*. This produced no significant change in performance (Figure S3A), suggesting that these neurons may function in parallel with other circuits to modulate memory. This is consistent with other behavioral effects of PPL2 neurons, which have typically been revealed by gain-of-function experiments (Kuo et al., 2015; Chen et al., 2017; Landayan et al., 2018; Sun et al., 2018). To determine whether PPL2 neurons affected reward learning, we carried out appetitive conditioning experiments and either blocked or stimulated PPL2 neurons during CS+ presentation (Figures S3B–S3E). Blocking PPL2 neurons during CS+ presentation had no effect on memory performance (Figures S3B and S3C). With transient activation of PPL2 neurons during CS+ presentation, there was a difference in performance between the experimental group and one of the controls but not the other (Figure S3E). However, a similar effect was observed when PPL2 neurons were unstimulated (Figure S3D). Thus, no effect could be attributed to manipulating PPL2 neurons in reward learning, suggesting that their role is either confined to aversive learning or masked by other factors, such as the starvation necessary to test reward learning.

We tested additional PPL2-innervating Gal4 drivers for memory enhancement (Figures S3F–S3J). Stimulation of PPL2 neurons with drivers that label smaller subsets of the cluster did not induce memory enhancement. Only the PPL2-Gal4 driver, which generates the strongest plasticity in the MB and labels the largest numbers of neurons (Figure S3J), enhanced behavioral memory. This suggests that memory enhancement requires strong activation of PPL2 neurons. Our data suggest that PPL2 neurons exert modulatory control over the MB, enhance the odor-evoked responses of MB neurons in an associative manner, and modulate aversive memory strength without innately encoding strong valence.

## DISCUSSION

This study provides insight into how PPL2 dopaminergic neurons regulate neuronal plasticity in the MB and behavioral learning. PPL2 neurons project to the MB calyx, where

intrinsic MB neurons receive input from olfactory projection neurons. This places them in a position to exert strong influence over MB olfactory responses. The present data suggest that they both act as a gain control that modulates the MB olfactory responses and increase the strength of aversive short-term memory. Activation of PPL2 neurons in a differential conditioning protocol increased the relative responsivity to the paired odor in  $\gamma$  neurons. Behaviorally, this did not drive memory on its own but increased the strength of memory if paired with odor-shock conditioning. Therefore, PPL2 neurons appear to modulate the strength of aversive memory, rather than dictating its content. One mechanism underlying this effect could be that PPL2 neurons enhance MB responses to the odor during training, facilitating the generation of synaptic plasticity that has been observed at the MB output synapses (Hige et al., 2015). The memory enhancement effect that we observed in flies may reflect a more general role that dopaminergic circuits play in other species. For instance, in mice, dopaminergic projections to the medial prefrontal cortex are not sufficient to induce memory, but they improve learning via effects on stimulus discrimination (Popescu et al., 2016).

Previous studies have suggested that PPL2 neurons could regulate motivation and arousal (Argue and Neckameyer, 2013; Kuo et al., 2015; Chen et al., 2017). Increased responses in the MB do not likely represent the valence of a memory directly, but they may reflect a salience or motivational component of memory. This is supported by PPL1 stimulation failing to induce changes in the odor representation in the MB but inducing conditioned aversion that drives heterosynaptic depression at certain MB-mushroom body output neuron (MBON) synapses (Hige et al., 2015). In contrast, PPL2 neurons drive strong  $\text{Ca}^{2+}$  response plasticity in the MB but do not encode strong valence on their own. The effect was limited to aversive memory, possibly because the starvation necessary for appetitive protocols had already maximized the animals' arousal state and/or salience of the sensory cues (though other possibilities are discussed later).

One function of PPL2 dopaminergic neurons may be to regulate the net responsivity of MB  $\gamma$  neurons to odorants and thereby alter the potential for stimuli to drive memory strength. Alternatively, the plasticity could regulate the balance of excitation across downstream MBONs that innervate spatially discrete zones of the MB and drive approach or avoidance behavior (Tanaka et al., 2008; Aso et al., 2014a, 2014b). For instance, increasing responses of MB  $\gamma$  neurons alone could increase the net excitatory drive to aversive MBONs relative to appetitive MBONs. In a previous study, we found that appetitive conditioning robustly increased  $\text{Ca}^{2+}$  responses to  $\text{CS}^+$  across the MB lobes (including both  $\gamma$  and  $\alpha/\beta$ ) (Louis et al., 2018). This could be interpreted to indicate either that the motivational component of appetitive conditioning differentially engages MB circuitry relative to aversive conditioning or that the appetitive valence is encoded as a bona fide cellular-level memory trace, comprising an increase in  $\text{Ca}^{2+}$  responses across all MB lobes. If the latter is true, perhaps a selective increase in  $\text{Ca}^{2+}$  responses in  $\gamma$  reflects a more aversive signature. Previous studies have demonstrated a critical role of  $\gamma$  neurons in short-term memory. Rescue of Rutabaga in the  $\gamma$  lobe of *rut* mutants is sufficient to restore performance in short-term memory (Zars et al., 2000; Blum et al., 2009; Trannoy et al., 2011), and rescue of the D1-like DopR receptor in the  $\gamma$  lobe is sufficient to rescue both short- and long-term memory (Qin et al., 2012). In

addition, aversive learning induces plasticity in synaptic vesicle release from the MB  $\gamma$  lobes (Zhang and Roman, 2013).

Several caveats in experimental interpretations should be noted. First, we do not know whether the MB plasticity forms in parallel to memory enhancement or directly drives it. Contributions of polysynaptic circuit elements to the physiological effects (MB plasticity) and/or behavioral effects (enhanced memory) are possible. Future mapping studies may identify additional circuit elements contributing to the memory networks underlying these phenomena. Nonetheless, anatomical innervation of the MB calyx by PPL2 neurons positions them to provide strong modulatory input to the MB dendrites and associated neuronal circuitry. Thus, while valence is layered at the MB output synapses (Séjourné et al., 2011; Plač ais et al., 2013; Aso et al., 2014b; Bouzaiane et al., 2015; Hige et al., 2015), our data suggest that PPL2 neurons may be a control mechanism that influences how responsive the MB is to odors, potentially altering the propensity for synaptic plasticity downstream.

## STAR★METHODS

### CONTACT FOR REAGENT AND RESOURCE SHARING

Further information and requests for resources and reagents should be directed to and will be fulfilled by the Lead Contact, Seth M. Tomchik (stomchik@scripps.edu).

### EXPERIMENTAL MODEL AND SUBJECT DETAILS

Flies were cultured according to standard methods and maintained on a 12:12 hr light:dark cycle. The fly stocks used in this work were TH-C'-Gal4,F-Gal80, TH-D'-Gal4 (Liu et al., 2012b), TH-Gal4 (Friggi-Grelin et al., 2003), Oc2-Gal4 (Blanco et al., 2011), NP3024-Gal4 (Kuo et al., 2015), NP5945-Gal4 (Kuo et al., 2015), murashka-1-Gal4 (Dubnau et al., 2003), UAS-TrpA1 (Hamada et al., 2008), and MB-GCaMP3 (Boto et al., 2014). TrpA1 crosses were kept at 23°C to avoid neuron activation during development. All fly lines were backcrossed R 6 generations into the Cantonized  $w^{1118}$  reference strain  $w^{CS10}$ .

### METHOD DETAILS

**Immunohistochemistry**—Five to seven day old fly brains were dissected in 1% paraformaldehyde in S2 medium, and processed according to a published protocol (Jenett et al., 2012). Briefly, brains were incubated with the primary antibodies for 3 hours at room temperature and at 4°C overnight, and with the secondary antibodies for 3 hours at room temperature and 4 days at 4°C. Incubations were performed in blocking serum (3% normal goat serum). After the final incubation and washes, brains were mounted in vectashield media for imaging. Immunostaining experiments were carried out with a UAS-GFP.nls (Bloomington #4776), which contains a nuclear localization signal but in neurons provides strong labeling of nuclei, somata, and neuronal processes. Antibodies used were rabbit anti-GFP (1:1000, Invitrogen), mouse anti-nc82 (1:50, DSHB), mouse anti-TH (1:200, Chemicon), goat anti-rabbit IgG and goat anti-mouse IgG (1:800, Alexa 488 or Alexa 633 respectively, Invitrogen). Images were obtained using Leica TCS SP8 confocal microscope.

**Functional imaging**—*In vivo* functional imaging was performed as described previously (Boto et al., 2014; Louis et al., 2018). Briefly, flies were immobilized in a custom-machined polycarbonate recording chamber that allows saline to flow across the dorsal head and thorax while keeping the rest of the fly dry. A small window was opened in the cuticle with a syringe needle to allow optical access to the brain, and saline was perfused at 2 ml/min. The odorants ethyl butyrate, isoamyl acetate, 3-octanol, or 4-methylcyclohexanol (Sigma-Aldrich) were delivered through a stainless steel pipette mounted 1 cm anterior to the fly's head, and presented for either 3 s (imaging) or 30 s (training). Air flow was 40–60 ml/min. The odorant was presented by switching the odor stream between scintillation vials containing either 1  $\mu$ L of odorant on filter paper or filter paper alone using solenoid valves (The Lee Co) controlled by a programmable logic controller (Omron). The odor/air streams were directed through PTFE (Teflon) tubing.

Baseline temperature in the recording chamber was held at 22°C. Temperature was controlled with an inline Peltier element (Warner Instruments) and monitored with a thermistor placed in the recording chamber adjacent to the fly's head. In differential conditioning experiments, where TrpA1 stimulation was paired with odor delivery, we ramped the temperature up from 22°C. When the bath temperature reached 24°C, the solenoid controlling CS+ odor delivery was activated to begin odor delivery immediately prior to reaching the TrpA1 activation threshold (27°C) (Viswanath et al., 2003). After 30 s, the temperature was ramped back down to 22°C. After a 30 s delay, the CS- was delivered for another 30 s. The total time between stimuli, including ramp time, was 1.5 min. During aversive conditioning protocols, the CS+ was presented for 30 s and paired with 3 electric shocks (60 V) of 1.25 s length with 8.75 s interval. The first shock was administered 8.75 s after the onset of odor stimulation. After a 2-minute rest interval, CS- was presented for 30 s.

Optical reporters were imaged with confocal microscopy on Leica TCS SP8 confocal microscopes at 256  $\times$  256 resolution. 488 nm excitation was paired with 500–600 nm bandpass emission filtration, acquired at 10 Hz.

**Behavioral Analysis**—Behavior was performed as previously described (Tomchik and Davis, 2009). Briefly, 2–5 day old flies were trained under dim red light at 22°C and ~75% relative humidity. Groups of ~60 flies were exposed for 1 min to an odor (CS+) paired with 6 shocks of 1.25 s each at 60V, followed by 30 s of air and 1 min of another odor (CS-). Depending on the protocol, flies were transferred to another chamber at 32°C for PPL2ab neuron stimulation at different time points during the behavior assay. The odor pairs were either ethyl butyrate and isoamyl acetate or 3-octanol and 4-methylcyclohexanol, with dilutions were adjusted so that naive flies equally avoided the two odors (0.05 – 0.1%). Memory was tested by inserting the trained flies in a T-maze in which they chose between an arm presenting the CS+ odor and an arm presenting the CS- odor across a 2 min choice period. The PI was measured immediately after training (~3 min). For odor and shock avoidance experiments, flies were allowed to choose between arms in a T-maze containing odor versus mineral oil (for odor avoidance) or an arm with a grid shocking the flies every 5 s at 60V versus an arm containing a non-electrified shock grid (shock avoidance). Appetitive conditioning experiments were performed in animals starved 16–20 h. Animals were

exposed for 2 min to an odor (CS+) at 32°C for TrpA1 stimulation (or 22°C in control experiments), paired with a 2M sucrose solution dried on filter paper, followed by 30 s of air and 2 min of another odor (CS-) (Krashes and Waddell, 2011). Memory was tested as described above.

## QUANTIFICATION AND STATISTICAL ANALYSIS

**Functional imaging**—Responses were plotted as the baseline-normalized change in GCaMP fluorescence ( $\Delta F/F$ ), averaged across a circumscribed region of interest. Statistical analysis was performed in MATLAB and Prism (Graphpad). Statistical significance (omnibus/post hoc) was determined using Mann-Whitney U tests (two groups, nonparametric) or Kruskal-Wallis/Dunn (one-way, nonparametric comparisons). For two-way comparisons, ANOVA/Sidak was used. Comparisons between pre and post-conditioning responses were made with the Wilcoxon rank sum test. We used the family-wise error rate  $\alpha_{FW} = 0.05$ .

Statistical details can be found in the figure legends and results section, where the  $n$  represents the number of flies used in the study (one data point per fly, except in Figures S1C–S1E, where the  $n$  represents the total number of cells pooled from four animals per condition). Boxplots graph the median as the central line, the box extending from the 25<sup>th</sup> to the 75<sup>th</sup> percentile, and the whiskers extending to the 10<sup>th</sup> and 90<sup>th</sup> percentiles.

**Behavioral analysis**—Memory was quantified by calculating the Performance Index (PI) as  $(\text{flies in the CS- arm}) - (\text{flies in the CS+ arm}) / (\text{total flies in both arms})$ . Avoidance indices were calculated as:  $[(\text{flies in the non-electrified arm}) - (\text{flies in the electrified arm})] / (\text{total flies analyzed})$ . Statistical significance (omnibus/post hoc) was determined using ANOVA (one-way parametric). Multiple comparisons within genotypes were conducted with Sidak's post hoc tests, using the family-wise error rate  $\alpha_{FW} = 0.05$ . P.I.s were compared to zero with a one-sample  $t$  test using Bonferroni correction for multiple comparisons.

## DATA AND SOFTWARE AVAILABILITY

Original data for this paper are deposited at <https://doi.org/10.17632/nssxb2fmmt.1>.

## Supplementary Material

Refer to Web version on PubMed Central for supplementary material.

## ACKNOWLEDGMENTS

We thank Qili Liu and Mark N. Wu, Ronald L. Davis, the Bloomington Drosophila Stock Center, and the Kyoto DGRC for fly stocks. Research support was provided by NIH/NIMH (R00 MH092294), NIH/NINDS (R01 NS097237), and the Whitehall Foundation. T.B. and T.L. were Neuroscience Scholars of the Esther B. O'Keeffe Charitable Foundation.

## REFERENCES

Argue KJ, and Neckameyer WS (2013). Sexually dimorphic recruitment of dopamine neurons into the stress response circuitry. *Behav. Neurosci* 127, 734–743. [PubMed: 24128361]

- Aso Y, Siwanowicz I, Bräcker L, Ito K, Kitamoto T, and Tanimoto H (2010). Specific dopaminergic neurons for the formation of labile aversive memory. *Curr. Biol* 20, 1445–1451. [PubMed: 20637624]
- Aso Y, Herb A, Ogueta M, Siwanowicz I, Templier T, Friedrich AB, Ito K, Scholz H, and Tanimoto H (2012). Three dopamine pathways induce aversive odor memories with different stability. *PLoS Genet* 8, e1002768. [PubMed: 22807684]
- Aso Y, Hattori D, Yu Y, Johnston RM, Iyer NA, Ngo TT, Dionne H, Abbott LF, Axel R, Tanimoto H, and Rubin GM (2014a). The neuronal architecture of the mushroom body provides a logic for associative learning. *eLife* 3, e04577. [PubMed: 25535793]
- Aso Y, Sitaraman D, Ichinose T, Kaun KR, Vogt K, Belliard-Guérin G, Plaçais PY, Robie AA, Yamagata N, Schnaitmann C, et al. (2014b). Mushroom body output neurons encode valence and guide memory-based action selection in *Drosophila*. *eLife* 3, e04580. [PubMed: 25535794]
- Berry JA, Cervantes-Sandoval I, Nicholas EP, and Davis RL (2012). Dopamine is required for learning and forgetting in *Drosophila*. *Neuron* 74, 530–542. [PubMed: 22578504]
- Blanco J, Pandey R, Wasser M, and Udolph G (2011). Orthodenticle is necessary for survival of a cluster of clonally related dopaminergic neurons in the *Drosophila* larval and adult brain. *Neural Dev* 6, 34. [PubMed: 21999236]
- Blum AL, Li W, Cressy M, and Dubnau J (2009). Short- and long-term memory in *Drosophila* require cAMP signaling in distinct neuron types. *Curr. Biol* 19, 1341–1350. [PubMed: 19646879]
- Boto T, Louis T, Jindachomthong K, Jalink K, and Tomchik SM (2014). Dopaminergic modulation of cAMP drives nonlinear plasticity across the *Drosophila* mushroom body lobes. *Curr. Biol* 24, 822–831. [PubMed: 24684937]
- Bouzaiane E, Trannoy S, Scheunemann L, Plaçais PY, and Preat T (2015). Two independent mushroom body output circuits retrieve the six discrete components of *Drosophila* aversive memory. *Cell Rep* 11, 1280–1292. [PubMed: 25981036]
- Chen SL, Chen YH, Wang CC, Yu YW, Tsai YC, Hsu HW, Wu CL, Wang PY, Chen LC, Lan TH, and Fu TF (2017). Active and passive sexual roles that arise in *Drosophila* male-male courtship are modulated by dopamine levels in PPL2ab neurons. *Sci. Rep* 7, 44595. [PubMed: 28294190]
- Claridge-Chang A, Roorda RD, Vrontou E, Sjulson L, Li H, Hirsh J, and Miesenböck G (2009). Writing memories with light-addressable reinforcement circuitry. *Cell* 139, 405–415. [PubMed: 19837039]
- Dubnau J, Chiang AS, Grady L, Barditch J, Gossweiler S, McNeil J, Smith P, Buldoc F, Scott R, Certa U, et al. (2003). The staufer/pumilio pathway is involved in *Drosophila* long-term memory. *Curr. Biol* 13, 286–296. [PubMed: 12593794]
- Friggi-Grelin F, Iché M, and Birman S (2003). Tissue-specific developmental requirements of *Drosophila* tyrosine hydroxylase isoforms. *Genesis* 35, 260–269. [PubMed: 12717737]
- Galili DS, Dylla KV, Lüdke A, Friedrich AB, Yamagata N, Wong JY, Ho CH, Szyszka P, and Tanimoto H (2014). Converging circuits mediate temperature and shock aversive olfactory conditioning in *Drosophila*. *Curr. Biol* 24, 1712–1722. [PubMed: 25042591]
- Gervasi N, Tchénio P, and Preat T (2010). PKA dynamics in a *Drosophila* learning center: coincidence detection by rutabaga adenylyl cyclase and spatial regulation by dunce phosphodiesterase. *Neuron* 65, 516–529. [PubMed: 20188656]
- Hamada FN, Rosenzweig M, Kang K, Pulver SR, Ghezzi A, Jegla TJ, and Garrity PA (2008). An internal thermal sensor controlling temperature preference in *Drosophila*. *Nature* 454, 217–220. [PubMed: 18548007]
- Hige T, Aso Y, Modi MN, Rubin GM, and Turner GC (2015). Heterosynaptic Plasticity Underlies Aversive Olfactory Learning in *Drosophila*. *Neuron* 88, 985–998. [PubMed: 26637800]
- Jenett A, Rubin GM, Ngo TT, Shepherd D, Murphy C, Dionne H, Pfeiffer BD, Cavallaro A, Hall D, Jeter J, et al. (2012). A GAL4-driver line resource for *Drosophila* neurobiology. *Cell Rep* 2, 991–1001. [PubMed: 23063364]
- Krashes MJ, and Waddell S (2011). *Drosophila* appetitive olfactory conditioning. *Cold Spring Harb. Protoc* 5, prot5609.

- Kuo SY, Wu CL, Hsieh MY, Lin CT, Wen RK, Chen LC, Chen YH, Yu YW, Wang HD, Su YJ, et al. (2015). PPL2ab neurons restore sexual responses in aged *Drosophila* males through dopamine. *Nat. Commun* 6, 7490. [PubMed: 26123524]
- Landayan D, Feldman DS, and Wolf FW (2018). Satiation state-dependent dopaminergic control of foraging in *Drosophila*. *Sci. Rep* 8, 5777. [PubMed: 29636522]
- Liu C, Plaçais PY, Yamagata N, Pfeiffer BD, Aso Y, Friedrich AB, Siwanowicz I, Rubin GM, Preat T, and Tanimoto H (2012a). A subset of dopamine neurons signals reward for odour memory in *Drosophila*. *Nature* 488, 512–516. [PubMed: 22810589]
- Liu Q, Liu S, Kodama L, Driscoll MR, and Wu MN (2012b). Two dopaminergic neurons signal to the dorsal fan-shaped body to promote wakefulness in *Drosophila*. *Curr. Biol* 22, 2114–2123. [PubMed: 23022067]
- Louis T, Stahl A, Boto T, and Tomchik SM (2018). Cyclic AMP-dependent plasticity underlies rapid changes in odor coding associated with reward learning. *Proc. Natl. Acad. Sci. USA* 115, E448–E457. [PubMed: 29284750]
- Mao Z, and Davis RL (2009). Eight different types of dopaminergic neurons innervate the *Drosophila* mushroom body neuropil: anatomical and physiological heterogeneity. *Front. Neural Circuits* 3, 5. [PubMed: 19597562]
- Matsumoto M, and Hikosaka O (2009). Two types of dopamine neuron distinctly convey positive and negative motivational signals. *Nature* 459, 837–841. [PubMed: 19448610]
- Plaçais PY, Trannoy S, Friedrich AB, Tanimoto H, and Preat T (2013). Two pairs of mushroom body efferent neurons are required for appetitive long-term memory retrieval in *Drosophila*. *Cell Rep* 5, 769–780. [PubMed: 24209748]
- Popescu AT, Zhou MR, and Poo MM (2016). Phasic dopamine release in the medial prefrontal cortex enhances stimulus discrimination. *Proc. Natl. Acad. Sci. USA* 113, E3169–E3176. [PubMed: 27185946]
- Qin H, Cressy M, Li W, Coravos JS, Izzi SA, and Dubnau J (2012). Gamma neurons mediate dopaminergic input during aversive olfactory memory formation in *Drosophila*. *Curr. Biol* 22, 608–614. [PubMed: 22425153]
- Riemensperger T, Völlner T, Stock P, Buchner E, and Fiala A (2005). Punishment prediction by dopaminergic neurons in *Drosophila*. *Curr. Biol* 15, 1953–1960. [PubMed: 16271874]
- Schroll C, Riemensperger T, Bucher D, Ehmer J, Völlner T, Erbguth K, Gerber B, Hendel T, Nagel G, Buchner E, and Fiala A (2006). Light-induced activation of distinct modulatory neurons triggers appetitive or aversive learning in *Drosophila* larvae. *Curr. Biol* 16, 1741–1747. [PubMed: 16950113]
- Schultz W (1997). Dopamine neurons and their role in reward mechanisms. *Curr. Opin. Neurobiol* 7, 191–197. [PubMed: 9142754]
- Schwaerzel M, Monastirioti M, Scholz H, Friggi-Grelin F, Birman S, and Heisenberg M (2003). Dopamine and octopamine differentiate between aversive and appetitive olfactory memories in *Drosophila*. *J. Neurosci* 23, 10495–10502. [PubMed: 14627633]
- Séjourné J, Plaçais PY, Aso Y, Siwanowicz I, Trannoy S, Thoma V, Tedjakumala SR, Rubin GM, Tchénio P, Ito K, et al. (2011). Mushroom body efferent neurons responsible for aversive olfactory memory retrieval in *Drosophila*. *Nat. Neurosci* 14, 903–910. [PubMed: 21685917]
- Sitaraman D, Zars M, Laferriere H, Chen YC, Sable-Smith A, Kitamoto T, Rottinghaus GE, and Zars T (2008). Serotonin is necessary for place memory in *Drosophila*. *Proc. Natl. Acad. Sci. USA* 105, 5579–5584. [PubMed: 18385379]
- Sun J, Xu AQ, Giraud J, Poppinga H, Riemensperger T, Fiala A, and Birman S (2018). Neural Control of Startle-Induced Locomotion by the Mushroom Bodies and Associated Neurons in *Drosophila*. *Front. Syst. Neurosci* 12, 6. [PubMed: 29643770]
- Tanaka NK, Tanimoto H, and Ito K (2008). Neuronal assemblies of the *Drosophila* mushroom body. *J. Comp. Neurol* 508, 711–755. [PubMed: 18395827]
- Tomchik SM, and Davis RL (2009). Dynamics of learning-related cAMP signaling and stimulus integration in the *Drosophila* olfactory pathway. *Neuron* 64, 510–521. [PubMed: 19945393]
- Trannoy S, Redt-Clouet C, Dura JM, and Preat T (2011). Parallel processing of appetitive short- and long-term memories in *Drosophila*. *Curr. Biol* 21, 1647–1653. [PubMed: 21962716]

- Turner GC, Bazhenov M, and Laurent G (2008). Olfactory representations by *Drosophila* mushroom body neurons. *J. Neurophysiol* 99, 734–746. [PubMed: 18094099]
- Viswanath V, Story GM, Peier AM, Petrus MJ, Lee VM, Hwang SW, Patapoutian A, and Jegla T (2003). Opposite thermosensor in fruitfly and mouse. *Nature* 423, 822–823. [PubMed: 12815418]
- Yamagata N, Ichinose T, Aso Y, Plaçais PY, Friedrich AB, Sima RJ, Preat T, Rubin GM, and Tanimoto H (2015). Distinct dopamine neurons mediate reward signals for short- and long-term memories. *Proc. Natl. Acad. Sci. USA* 112, 578–583. [PubMed: 25548178]
- Zars T, Fischer M, Schulz R, and Heisenberg M (2000). Localization of a short-term memory in *Drosophila*. *Science* 288, 672–675. [PubMed: 10784450]
- Zhang S, and Roman G (2013). Presynaptic inhibition of gamma lobe neurons is required for olfactory learning in *Drosophila*. *Curr. Biol* 23, 2519–2527. [PubMed: 24291093]

### Highlights

- Two sets of dopaminergic neurons independently regulate memory encoding and strength
- Dendrite-innervating PPL2 neurons regulate  $\text{Ca}^{2+}$  responses in memory-encoding neurons
- PPL1 neurons drive aversive reinforcement (valence)
- PPL2 neurons enhance memory strength without driving valence

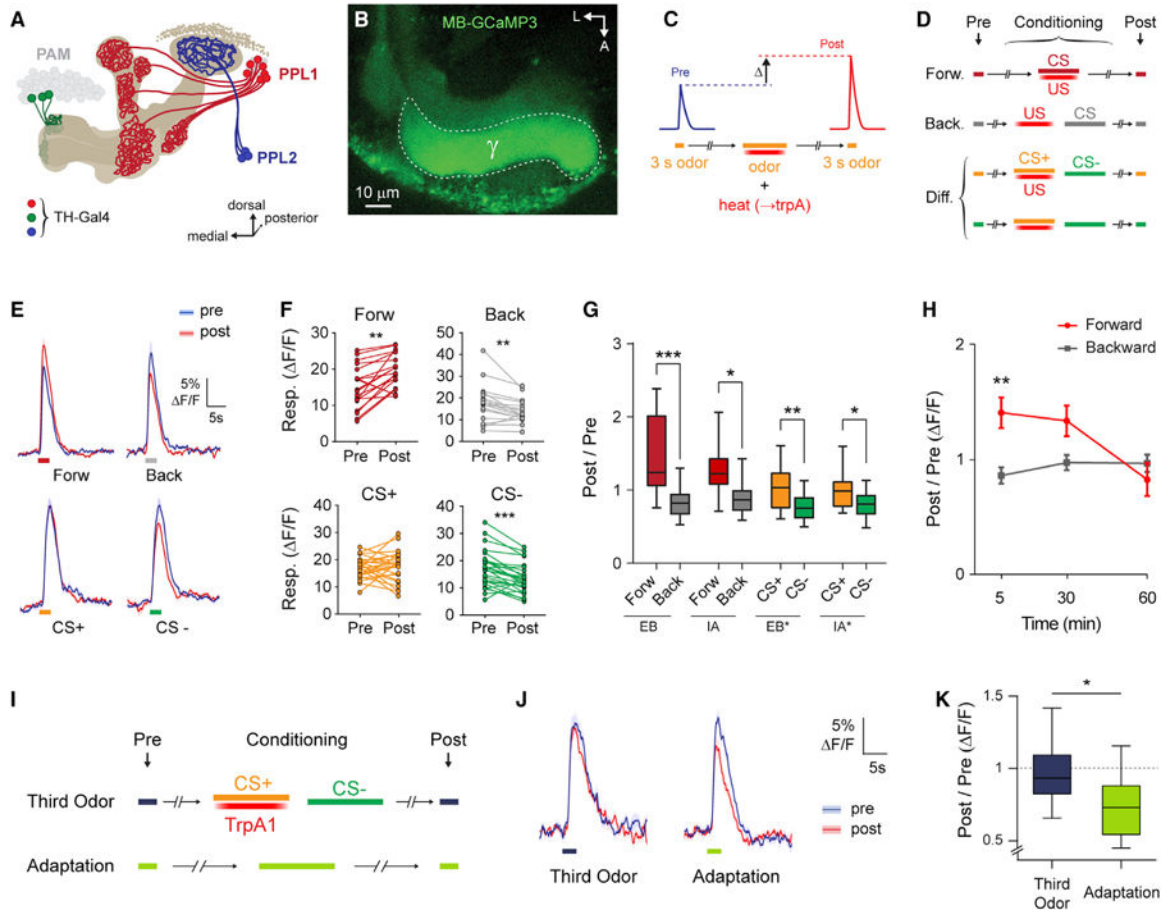


**Figure 1. Stimulation of Dopaminergic Neurons Increases MB Responses to Trained Odors**

(A) MB-innervating dopaminergic clusters labeled by TH-Gal4.

(B) GCaMP fluorescence in an MB-GCaMP3 fly. A region of interest was drawn around the MB g lobe. A, anterior; L, lateral.

(C) General experimental protocol.

(D) Variations on the experimental protocol. Forw, forward; Back, backward; Diff, differential.

(E) GCaMP responses (mean  $\pm$  SEM) to odors in TH > TrpA1; MB-GCaMP3 flies. Odor responses before and after conditioning are marked pre (blue) and post (red). Traces correspond to protocols in (D). Ethyl butyrate (EB) was used for Forw, Back, and CS+. Isoamyl acetate (IA) was used as CS-. Shaded bars represent odor delivery duration.

(F) Pre- and post-conditioning responses for each fly (\*\* $p < 0.01$ , \*\*\* $p < 0.001$ , Wilcoxon rank-sum test;  $n = 19$ ).

(G) Post-/pre-conditioning response ratio in the  $\gamma$  lobe ( $n = 13$ ). The asterisk in the legend indicates the odor that was used as CS+ (EB\* and IA\*). There was a significant effect across groups ( $p < 0.01$ , Kruskal-Wallis; \* $p < 0.05$ , \*\* $p < 0.01$ , \*\*\* $p < 0.001$ , Dunn).

(H) Time course of the effect comparing forward and backward protocols. There was significant interaction between protocols across time (\* $p < 0.05$ , two-way ANOVA; \*\* $p < 0.01$ , Sidak's multiple comparisons;  $n = 11$ ).

(I) Protocols used to establish the baseline responses of nonreinforced odors.

(J) GCaMP3 responses (mean  $\pm$  SEM) in the g lobe to 3-octanol not included in the associative protocol (left) and 3-octanol before and after a 30 s exposure (right). Odor responses imaged before and after the adaptation protocol or third odor protocol are marked pre (blue) and post (red). Shaded bars indicate odor delivery duration.

(K) Post-/pre-odor response ratio in the g lobe for the protocols in (I) ( $p = 0.016$ , Mann-Whitney;  $n = 12-13$ ).

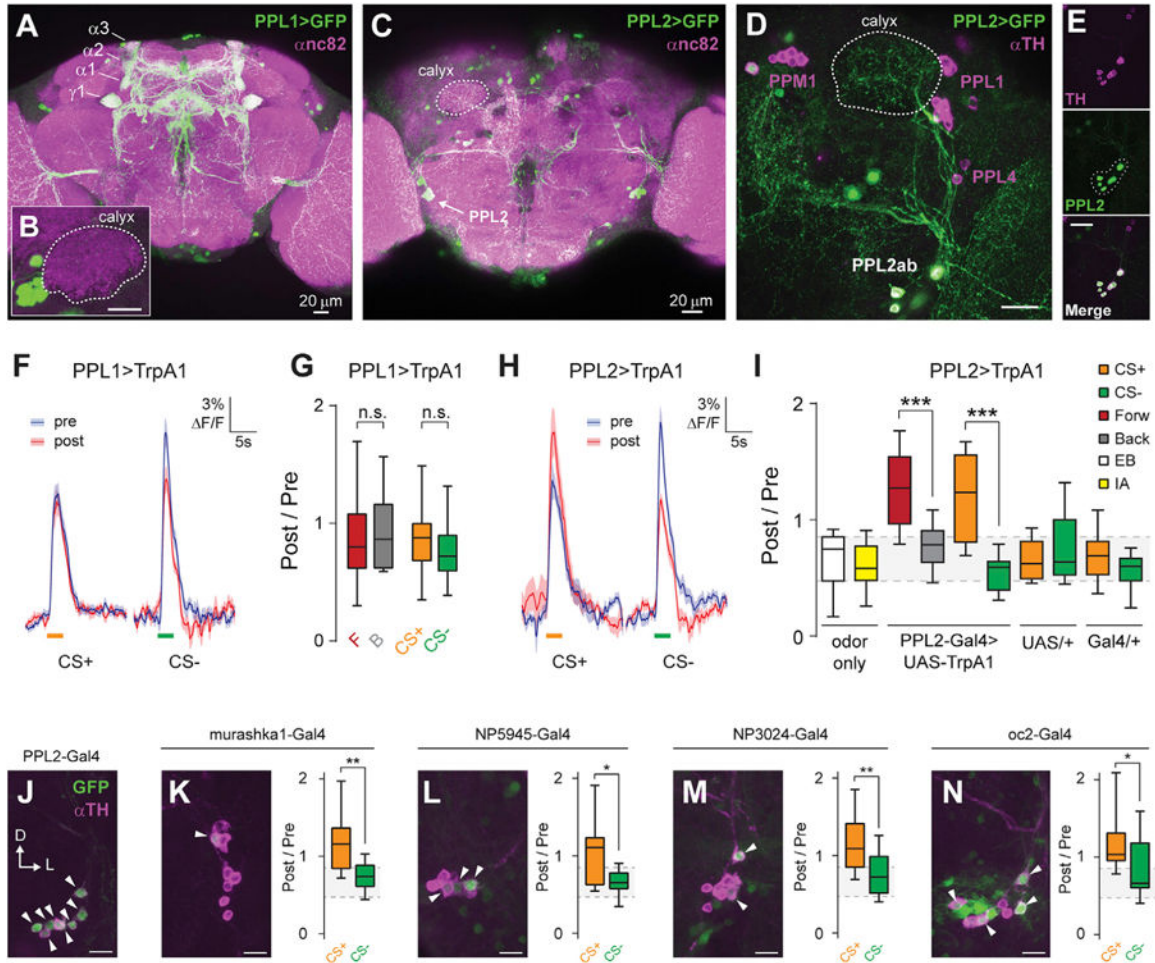


**Figure 2. Dopaminergic Plasticity Maps to PPL2 Neurons, Rather Than PPL1**

(A) Maximum intensity projection of anti-GFP (green) and anti-nc82 (magenta) immunostaining of the brain of a PPL1-Gal4 > UAS-GFP fly.

(B) Inset showing lack of innervation of the calyx. Scale bar, 20 μm.

(C) Maximum intensity projection of anti-GFP (green) and anti-nc82 (magenta) immunostaining of the posterior brain of a PPL2-Gal4 > UAS-GFP fly.

(D) Maximum intensity projection of anti-GFP (green) and anti-TH (magenta) immunostaining of a PPL2-Gal4 > UAS-GFP fly, showing terminal projections of PPL2ab neurons in the MB calyx (outlined with a dotted white line). Scale bar, 20 μm.

(E) PPL2-Gal4 driver labeling all TH-immunopositive neurons in the PPL2 cluster, as shown by complete overlap between GFP and TH staining in the PPL2 cell bodies (dotted outline in GFP image). Scale bar, 20 μm.

(F) Odor responses (mean ± SEM) in PPL1-Gal4 > UAS-TrpA1; MB-GCaMP3 flies. EB was presented as CS+. IA was presented as CS—. Shaded bars represent odor delivery duration.

(G) Post-/pre-odor response ratio in the g lobe when activation of PPL1 neurons was paired with odor exposure (p > 0.05, Dunn’s post hoc comparisons; n = 12–18).

(H) Odor responses (mean  $\pm$  SEM) in PPL2-Gal4 > UAS-TrpA1; MB-GCaMP3 flies. EB was presented as CS+. IA was presented as CS—. Shaded bars represent odor delivery duration.

(I) Post-/pre-odor response ratio in the g lobe when activation of PPL2 neurons was paired with odor exposure (n = 12). There was a significant effect across groups (p < 0.01, Kruskal-Wallis). Post hoc comparisons were performed between forward and backward protocols and between CS+ and CS— responses for the labeled genotypes. The gray shading indicates the inter-quartile range of the odor-only controls (\*\*p < 0.001, Dunn).

(J) Maximum intensity projection of anti-GFP (green) and anti-TH (magenta) immunostaining of the PPL2 somata from a PPL2-Gal4 > UAS-GFP fly. Arrowheads indicate cells positive for both TH and GFP. Scale bar, 10  $\mu$ m.

(K–N) Immunostaining of additional PPL2-Gal4 drivers (K: murashka1-Gal4; L: NP5945-Gal4; M: NP3024-Gal4; N: oc2-Gal4) (left), and effect of pairing stimulation of PPL2 neurons with odor exposure in a conditioning paradigm (right), as in (I). n = 12 for each genotype and condition. Scale bars, 10 mm (\*p < 0.05, \*\*p < 0.01, Mann-Whitney).

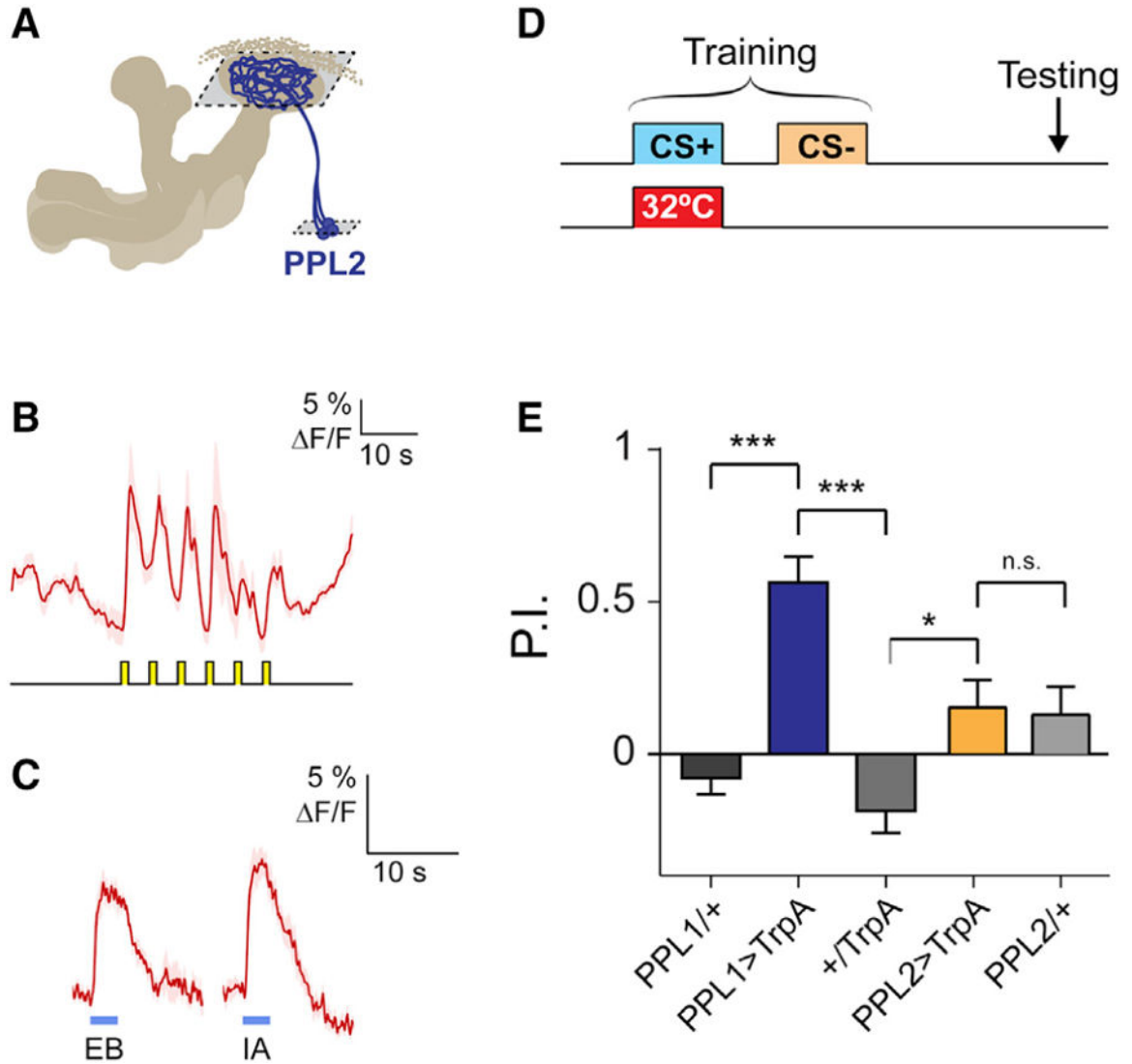


**Figure 3. PPL2 Neurons Respond to Odor and Shock but Do Not Encode Valence**

(A) Schematic of PPL2 projections to the MB. PPL2 neurons were imaged in focal planes through the calyx and cell body layers (outlined with dashed boxes).

(B) Shock responses in PPL2 somata (mean  $\pm$  SEM) to 6 pulses of 60 V (n = 4).

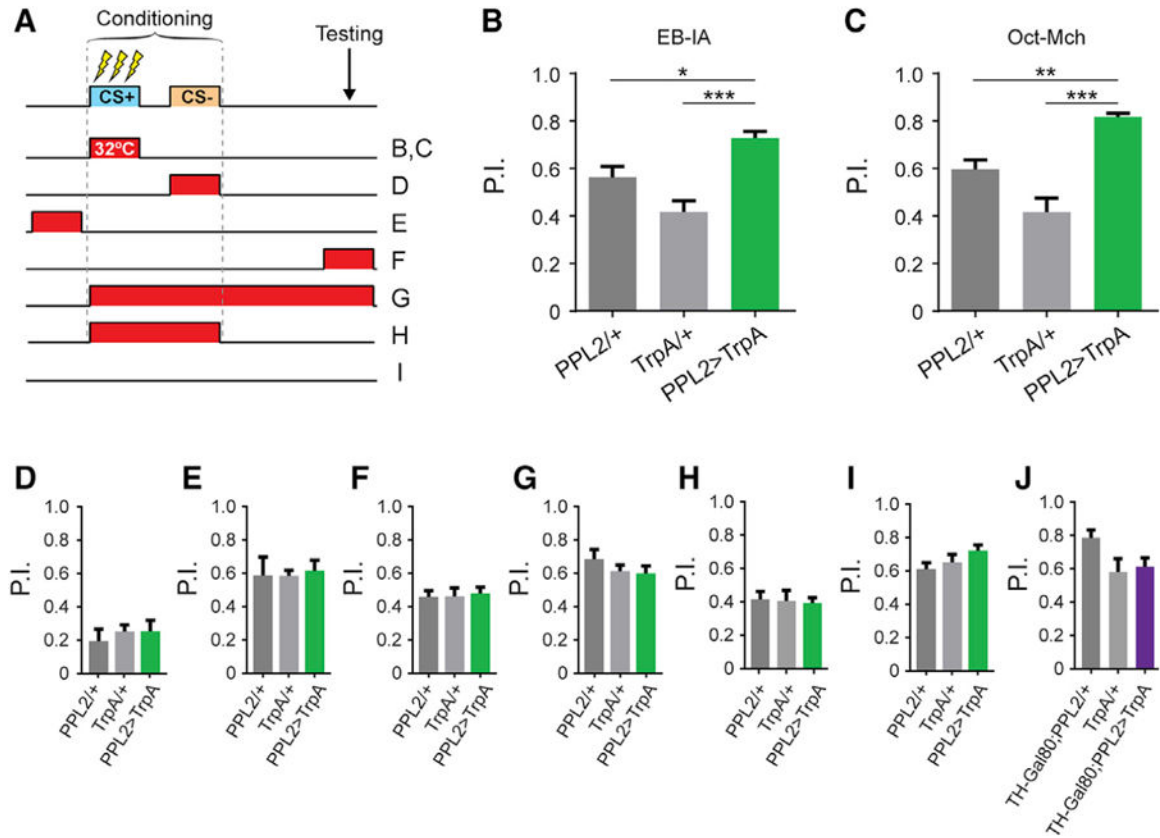
(C) Odor responses of PPL2 neurons to EB and IA in the calyces (mean  $\pm$  SEM; n > 6).

Shaded bars represent odor delivery duration.

(D) Protocol for testing the valence effect of dopaminergic neurons. TrpA1 was expressed in either PPL1 or PPL2 neurons, and neural activation was paired with odor in the absence of a reinforcer.

(E) Avoidance induced by transient activation of dopaminergic neurons, as in (D) (n = 6).

There was a significant effect across groups (p < 0.001, ANOVA; \*\*\*p < 0.001, \*p < 0.05, Sidak). Only the PPL1 > TrpA1 group significantly differed from zero (p < 0.01, one-sample t test).



## KEY RESOURCES TABLE

REAGENT or RESOURCE	SOURCE	IDENTIFIER
<b>Antibodies</b>		
GFP	Life Technologies	Cat # A11122; RRID: AB_221569
nc82	DSHB	AB_2314866
TH	Chemicon	Cat # MAB318; RRID: AB_2201528
Goat anti rabbit – Alexa 488	Life Technologies	Cat # A11008; RRID: AB_143165
Goat anti mouse – Alexa 633	Life Technologies	Cat # A21052; RRID: AB_2535719
<b>Deposited Data</b>		
Raw original data	This paper	<a href="https://doi.org/10.17632/nssxb2fmmt.1">https://doi.org/10.17632/nssxb2fmmt.1</a>
<b>Experimental Models: Organisms/Strains</b>		
DTH-C <sup>1</sup> -Gal4,F-Gal80	Mark Wu Lab	Liu et al., 2012b
DTH-D <sup>1</sup> -Gal4	Mark Wu Lab	Liu et al., 2012b
TH-Gal4	Ron Davis Lab	Friggi-Grelin et al., 2003
Oc2-Gal4	Jorge Blanco	Blanco et al., 2011
NP3024-Gal4	Kyoto Stock Center DGRC	#113066
NP5945-Gal4	Kyoto Stock Center DGRC	#105062
murashka-1-Gal4	Josh Dubnau Lab	Dubnau et al., 2003
UAS-TrpA1	Paul Garrity Lab	Hamada et al., 2008
MB-GCaMP3	Seth Tomchik Lab	Boto et al., 2014
UAS-mCD8::GFP	Bloomington Drosophila Stock Center	#32195
<b>Software and Algorithms</b>		
ImageJ		<a href="https://imagej.nih.gov/ij/">https://imagej.nih.gov/ij/</a>
MATLAB 2015b	MathWorks	<a href="https://www.mathworks.com/products/matlab.html">https://www.mathworks.com/products/matlab.html</a>
Prism 6.07	GraphPad	<a href="https://www.graphpad.com/">https://www.graphpad.com/</a>
Leica Application Suit X (LASX)	Leica Microsystems	<a href="https://www.leica-microsystems.com">https://www.leica-microsystems.com</a>